npg

## ORIGINAL ARTICLE

# Identification of LDH-A as a therapeutic target for cancer cell killing via (i) p53/NAD(H)-dependent and (ii) p53-independent pathways

SJ Allison[1,2], JRP Knight[1,4], C Granchi[3], R Rani[3], F Minutolo[3], J Milner[1] and RM Phillips[2]

Most cancer cells use aerobic glycolysis to fuel their growth. The enzyme lactate dehydrogenase-A (LDH-A) is key to cancer's glycolytic phenotype, catalysing the regeneration of nicotinamide adenine dinucleotide (NAD$^+$) from reduced nicotinamide adenine dinucleotide (NADH) necessary to sustain glycolysis. As such, LDH-A is a promising target for anticancer therapy. Here we ask if the tumour suppressor p53, a major regulator of cellular metabolism, influences the response of cancer cells to LDH-A suppression. LDH-A knockdown by RNA interference (RNAi) induced cancer cell death in p53 wild-type, mutant and p53-null human cancer cell lines, indicating that endogenous LDH-A promotes cancer cell survival irrespective of cancer cell p53 status. Unexpectedly, however, we uncovered a novel role for p53 in the regulation of cancer cell NAD$^+$ and its reduced form NADH. Thus, LDH-A silencing by RNAi, or its inhibition using a small-molecule inhibitor, resulted in a p53-dependent increase in the cancer cell ratio of NADH:NAD$^+$. This effect was specific for p53$^{+/+}$ cancer cells and correlated with (i) reduced activity of NAD$^+$-dependent deacetylase sirtuin 1 (SIRT1) and (ii) an increase in acetylated p53, a known target of SIRT1 deacetylation activity. In addition, activation of the redox-sensitive anticancer drug EO9 was enhanced selectively in p53$^{+/+}$ cancer cells, attributable to increased activity of NAD(P)H-dependent oxidoreductase NQO1 (NAD(P)H quinone oxidoreductase 1). Suppressing LDH-A increased EO9-induced DNA damage in p53$^{+/+}$ cancer cells, but importantly had no additive effect in non-cancer cells. Our results identify a unique strategy by which the NADH/NAD$^+$ cellular redox status can be modulated in a cancer-specific, p53-dependent manner and we show that this can impact upon the activity of important NAD(H)-dependent enzymes. To summarise, this work indicates two distinct mechanisms by which suppressing LDH-A could potentially be used to kill cancer cells selectively, (i) through induction of apoptosis, irrespective of cancer cell p53 status and (ii) as a part of a combinatorial approach with redox-sensitive anticancer drugs via a novel p53/NAD(H)-dependent mechanism.

## INTRODUCTION

Cancer and non-cancer cells differ fundamentally in their metabolism.[1] Many cancer cells are reprogrammed to utilise glycolysis rather than mitochondrial oxidative phosphorylation as their major source of energy for cell growth and proliferation.[2–4] Reliance on glycolysis even in the presence of oxygen (the Warburg effect) appears to be directly linked to the activation of oncogenes and loss of tumour suppressors,[5,6] leading to a resurgence of interest in its role in cancer development.

The enzyme lactate dehydrogenase (LDH) is pivotal in ensuring there is enough nicotinamide adenine dinucleotide (NAD$^+$) to fuel cancer cell glycolysis. LDH is a tetrameric enzyme composed of two different subunits (LDH-A and LDH-B) encoded by separate genes. LDH catalyses the interconversion of pyruvate and reduced nicotinamide adenine dinucleotide (NADH) generated by glycolysis to lactate and NAD$^+$. The direction of catalysis depends on the proportion of LDH-A and LDH-B in the LDH complex; LDH-A promotes reduction of pyruvate to lactate to regenerate NAD$^+$ from NADH, whereas LDH-B favours the reverse reaction.[7,8]

Through regenerating the NAD$^+$ required to drive glycolysis in cancer cells, LDH-A is a key enzyme involved in the Warburg effect and in sustaining cancer's glycolytic phenotype. Non-cancer cells utilise oxidative phosphorylation in the presence of oxygen to generate energy; under such conditions, LDH-A is presumed dispensable, only being required for anaerobic glycolysis when oxygen is sparse. Significantly, LDH-A suppression has been reported to reduce cellular transformation and inhibit tumour progression.[9–11]

LDH-A inhibition has the potential to alter the cellular balance between NAD$^+$ and its reduced form NADH. Perturbation of the cellular NADH/NAD$^+$ ratio, as well as potentially inhibiting aerobic glycolysis, could impact upon other cellular processes and enzymes, which utilise NAD$^+$ and NADH. The role of NAD(H) as a cofactor in oxidation/reduction reactions is well established and the activity of NAD(H)-dependent enzymes appear sensitive to cellular changes in NAD(H).[12–14] Many of these enzymes have important biological and therapeutic functions. For example, the oxidoreductase NAD(P)H quinone oxidoreductase 1 (NQO1)

[1]Department of Biology, University of York, York, UK; [2]Institute of Cancer Therapeutics, University of Bradford, Bradford, UK and [3]Dipartimento di Farmacia, Università di Pisa, Pisa, Italy. Correspondence: Dr SJ Allison, Institute of Cancer Therapeutics, University of Bradford, Tumbling Hill Street, Bradford, North Yorkshire BD7 1DP, UK.
E-mail: s.allison1@bradford.ac.uk
[4]Current address: MRC Toxicology Unit, University of Leicester, Leicester, UK.

utilises NADH to reduce the quinone-based anticancer prodrug EO9 (Apaziquone) to cytotoxic metabolites.[15–17] In another example, NAD$^+$ is an essential cosubstrate for the sirtuin (SIRT) family of NAD$^+$-dependent protein deacetylases.[18] SIRT1, the most extensively studied of the human SIRTs, appears to be required for survival of certain cancer cells.[19–22] Disruption of NAD$^+$ biosynthetic pathways to reduce the activity of NAD$^+$-dependent enzymes such as SIRT1 is a therapeutic strategy being evaluated.[13] However, non-cancer cells also require NAD$^+$ for normal cell functions and this approach carries a risk of toxicity to normal cells.[23] Strategies designed to modulate NADH/NAD$^+$ selectively in cancer cells are required and one potential approach is targeting LDH-A. Thus by targeting LDH-A, this could potentially provide a way of reducing SIRT1 activity selectively in cancer cells. Among the many cellular substrates of SIRT1 is the tumour suppressor p53.[24,25] Targeting LDH-A could therefore, via SIRT1, indirectly provide a way of altering p53 acetylation status and the downstream induction of p53 target genes (e.g. *p21*) selectively in cancer cells. This is important as these genes have an important role in the p53 cellular stress response and the cellular decision as to whether to live, arrest or die.[26]

In addition to the key role of the tumour suppressor p53 as a cellular stress sensor and in the induction of growth arrest, senescence or apoptosis in response to DNA damage, it also influences multiple aspects of cellular metabolism as well as the cellular response to metabolic stress.[6,27] P53 regulates glycolysis, the pentose phosphate pathway, oxidative phosphorylation and glutaminolysis and its loss promotes the Warburg effect.[6] Here we ask if p53 influences the response of cancer cells to LDH-A suppression and its therapeutic potential. Using RNA interference (RNAi) and a panel of human cancer cell lines, we show that (i) LDH-A promotes cancer cell survival irrespective of cancer cell p53 status under normal growth conditions, whereas LDH-B appears non-essential, (ii) targeting LDH-A provides a p53-dependent mechanism by which the NADH:NAD$^+$ balance in cancer cells, but not that in non-cancer cells, can be significantly altered, (iii) LDH-A suppression reduces the activity of NAD$^+$-dependent deacetylase SIRT1 in p53$^{+/+}$ cancer cells and (iv) silencing LDH-A causes a p53-dependent increase in cancer cell sensitivity to the redox-dependent anticancer prodrug EO9, attributable to increased activity of NAD(P)H-dependent oxidoreductase NQO1. We further show that a small-molecule inhibitor of LDH-A, methyl 1-hydroxy-6-phenyl-4-(trifluoromethyl)-1*H*-indole-2-carboxylate (NHI-2),[28] is able to recapitulate many of these effects.

## RESULTS

### Selective knockdown of LDH-A and LDH-B
Efficient, selective mRNA knockdown of LDH-A and LDH-B by their respective small interfering RNAs (siRNAs) was observed, as determined by qRT-PCR (Figure 1a). LDH-A silencing had no effect on LDH-B mRNA levels and *vice versa* (Figure 1a). Similar mRNA knockdown efficiency was evident in human HCT116 cancer and ARPE19 non-cancer cell lines (Figure 1a).

Interestingly, the relative protein expression levels of LDH-A and LDH-B differed between the HCT116 cancer cells and the ARPE19 and WI38 non-cancer cell lines (Figure 1b). In the HCT116 cells, LDH-A and LDH-B protein levels were similar, whereas in the ARPE19 and WI38 cells, LDH-A protein levels were higher relative to LDH-B (Figure 1b). Nonetheless, LDH-A silencing resulted in an efficient knockdown of LDH-A protein in all cell lines (Figure 1b). LDH-B silencing efficiently depleted LDH-B protein and also caused some reduction in LDH-A protein levels, an effect not observed at the mRNA level (Figures 1a and b), implying increased LDH-A protein turnover in the absence of LDH-B. Control siRNAs targeting lamin A/C or SIRT1 had no effect on LDH-A or LDH-B levels (Figure 1b and Supplementary Figure S1a).

### LDH-A but not LDH-B depletion induces apoptosis in p53$^{+/+}$, mutant and p53$^{-/-}$ cancer cells
LDH-A silencing induced apoptosis in HCT116 cancer cells, both in p53$^{+/+}$ cells and in isogenic p53$^{-/-}$ cells, although to a lesser extent in the latter (Figures 1c and d). A second siRNA designed to target LDH-A also induced apoptosis (Supplementary Figure S2). In contrast, in the human non-cancer ARPE19 and WI38 cell lines, LDH-A silencing had no effect on cell viability (Figures 1c and d). LDH-A silencing also induced apoptosis in MCF7 breast cancer cells (p53 wild-type) and in the p53-mutant cancer cell lines MDA-MB-231, MDA-MB-468 and DLD1 (Figure 1d). Our results suggest that LDH-A promotes cancer cell survival irrespective of p53 status. Silencing LDH-B had no apparent effect on cell survival of any of the cell lines (Figures 1c and d).

### LDH-A suppression increases cancer cell NADH:NAD$^+$ and the effect is p53-dependent
As LDH-A catalyses the regeneration of NAD$^+$ from NADH, we hypothesised that LDH-A silencing may result in depletion of cellular NAD$^+$ and perturbation of the cellular redox balance of NADH:NAD$^+$. This can have lethal consequences for the cell as demonstrated by inhibition of the NAD$^+$ biosynthetic enzyme nicotinamide phosphoribosyltransferase (NAMPT).[13] Indeed, RNAi-mediated knockdown of NAMPT induces cell death in both HCT116 cancer cells and ARPE19 non-cancer cells (data not shown). Effects of LDH-A silencing upon NAD$^+$ and NADH were therefore determined. Thirty hours after transfection, LDH-A silencing caused a significant twofold increase in the cellular NADH:NAD$^+$ ratio in HCT116 p53$^{+/+}$ cancer cells (Figure 2a). LDH-B and lamin A/C silencing had no effect on NADH:NAD$^+$. In contrast to the twofold increase in NADH:NAD$^+$ observed in the p53$^{+/+}$ cancer cells, unexpectedly LDH-A silencing in the isogenic p53$^{-/-}$ cells did not cause a significant change in the cellular NADH:NAD$^+$ ratio despite equivalent LDH-A protein knockdown in the two cell lines (Figure 1b). This suggests that apoptosis induced by LDH-A silencing in the p53$^{-/-}$ cancer cells is not caused by changes in cellular NADH/NAD$^+$.

Importantly, the effects of LDH-A silencing on the cellular NADH/NAD$^+$ ratio in the isogenic p53$^{+/+}$ and p53$^{-/-}$ cancer cells were mimicked by suppressing LDH-A using a selective small-molecule inhibitor of LDH-A (Figure 2b). The LDH-A inhibitor used was NHI-2 (methyl 1-hydroxy-6-phenyl-4-(trifluoromethyl)-1*H*-indole-2-carboxylate).[28] NHI-2, a derivative of the *N*-hydroxyindole-2-carboxylate LDH-A inhibitors reported in 2011,[29] is a potent, selective LDH-A inhibitor with a half-maximal inhibitory concentration (IC$_{50}$) of 10.5 μM and a 4–5-fold LDH-A/LDH-B selectivity.[28] NHI-2 caused a significant increase in the cellular NADH/NAD$^+$ ratio of HCT116 p53$^{+/+}$ cells, but had no effect in the isogenic p53$^{-/-}$ cells (Figure 2b). Significantly, however, HCT116 p53$^{-/-}$ cells transiently transfected to express wild-type p53 showed an increase in the cellular NADH/NAD$^+$ ratio in response to NHI-2, confirming p53 dependency of the effect (Figure 2b). NHI-2 also increased the NADH/NAD$^+$ ratio in two other p53 wild-type cancer cell lines tested, LoVo and LS174, but it failed to have any effect in SiHa or SAOS2 cells, which are functionally p53-null (Figure 2b).

### LDH-B silencing decreases the NADH/NAD$^+$ ratio in ARPE19 and WI38 cells
In ARPE19 and WI38 non-cancer cells, LDH-A silencing did not increase the cellular NADH/NAD$^+$ ratio (Figure 2a). Interestingly, however, LDH-B silencing caused a decrease in the NADH/NAD$^+$ ratio in both the ARPE19 and WI38 cells (Figure 2a), an effect not observed in the HCT116 cancer cells. This suggests that LDH-B is the functionally dominant LDH isoform in ARPE19 and WI38 non-cancer cells and may have an active role in inhibiting aerobic glycolysis and promoting pyruvate entry into the tricarboxylic acid (TCA) cycle.
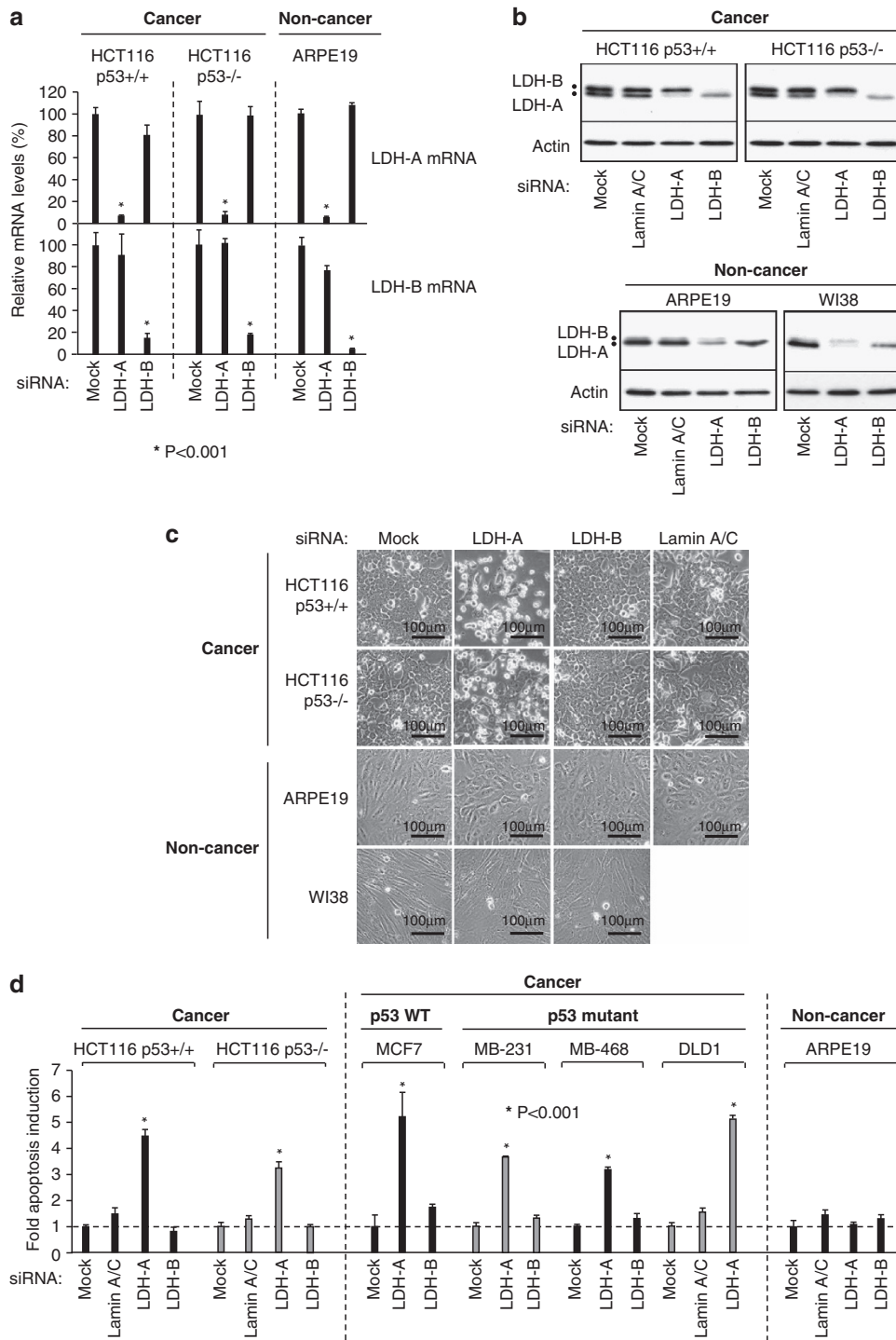
**Figure 1.** LDH-A promotes human cancer cell survival irrespective of cancer cell p53 status, but appears dispensable for viability in non-cancer cells. (**a**) LDH-A and LDH-B mRNA levels in HCT116 p53$^{+/+}$ and p53$^{-/-}$ cancer cells and in ARPE19 non-cancer cells 48 h after transfection with the indicated siRNA. Real-time polymerase chain reaction data (mean ± s.d. of four mRNA determinations). Statistical significance ($P < 0.001$) in LDH-A and LDH-B mRNA levels between silenced cells and control cells is indicated by an asterisk. (**b**) Immunoblots showing protein expression of LDH-A and LDH-B in HCT116 p53$^{+/+}$ and p53$^{-/-}$ cells (top) and ARPE19 and WI38 cells (bottom), and effects of the indicated siRNAs 30 h after siRNA transfection. Actin acts as a loading control. (**c**) Phase-contrast images of HCT116 p53$^{+/+}$ and p53$^{-/-}$ cells and ARPE19 and WI38 cells 72 h after transfection with the indicated siRNAs. Scale bar, 100 μm. (**d**) Fold induction of apoptosis relative to mock-transfected cells 72 h after siRNA transfection, as determined by annexin V labelling. Values represent early apoptotic cells that stain positive for annexin V and negative for propidium iodide (mean ± s.d. of three independent determinations). Statistical significance ($P < 0.001$) between LDH-A-silenced cells and control cells is indicated by an asterisk.
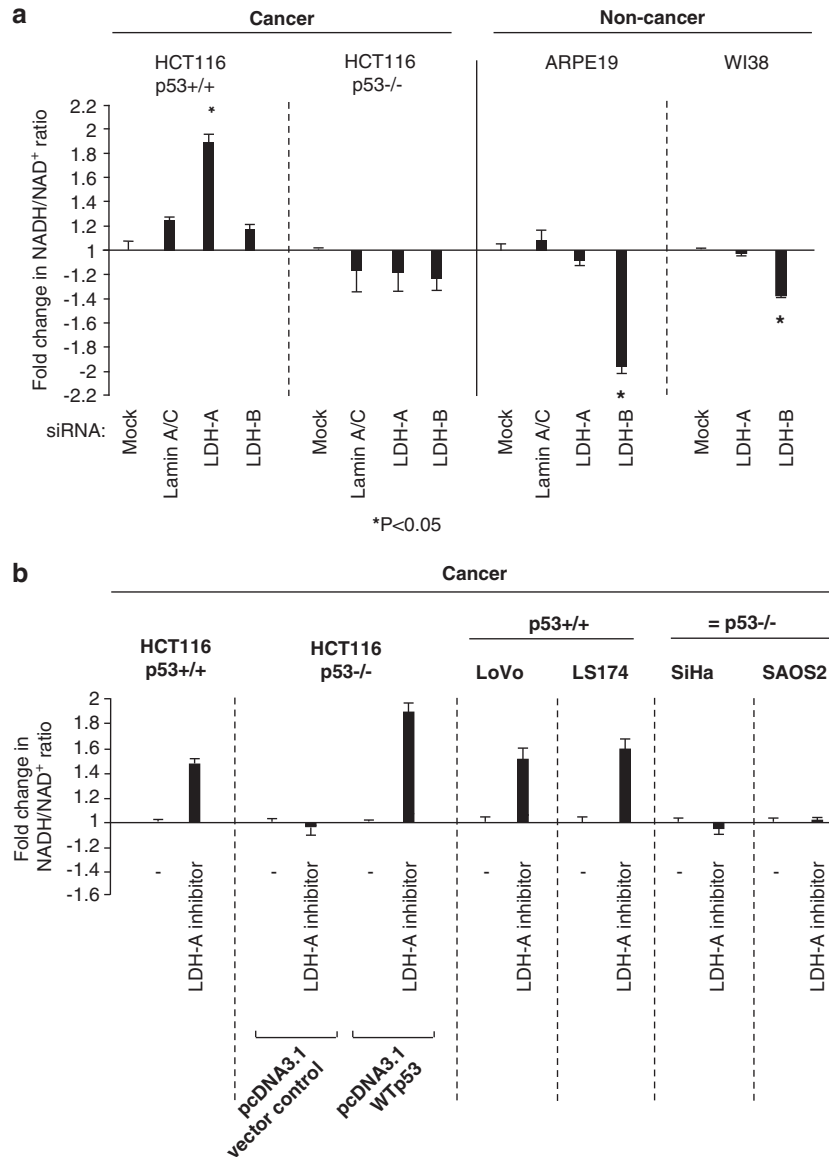
**Figure 2.** LDH-A suppression increases the cellular NADH:NAD$^+$ ratio in p53$^{+/+}$ cancer cells, but not in p53$^{-/-}$ cancer cells or ARPE19 and WI38 non-cancer cells. (**a**) Fold-change in the cellular NADH:NAD$^+$ ratio in HCT116 p53$^{+/+}$ and p53$^{-/-}$ cells and ARPE19 and WI38 cells 30 h after transfection with the indicated siRNAs. Fold-change $\pm$ s.d. from a minimum of three independent experiments. (**b**) Effect of LDH-A inhibitor NHI-2 (12.5 μM, 1h30) or dimethyl sulfoxide (DMSO) control on the cellular NADH:NAD$^+$ ratio in p53 wild-type or p53-null cancer cell lines. SiHa cells are functionally p53-null owing to the expression of HPV16 E6 (see Materials and methods section). Effect of expression of wild-type p53 by transient transfection in HCT116 p53$^{-/-}$ cells on the cellular response in NADH:NAD$^+$ to LDH-A inhibitor or DMSO control is also shown (pcDNA3.1 vector control versus pcDNA3.1 WTp53).

### Effect of p53 upon the cellular metabolic response to LDH-A silencing

The p53 dependency of the increase in cancer cell NADH:NAD$^+$ following LDH-A targeting suggests that p53 status may affect how the cells respond metabolically to LDH-A suppression. Using the HCT116 isogenic clones of p53$^{+/+}$ and p53$^{-/-}$ cancer cells, the influence of p53 upon glycolysis and oxidative metabolism following LDH-A silencing was analysed. Lactate release into the cell culture medium was determined as a measure of aerobic glycolysis. Under normal growth conditions, the p53$^{-/-}$ cells showed higher lactate release into the medium (Figure 3a), consistent with p53-mediated suppression of the Warburg effect.[6,30] Thirty hours after LDH-A silencing, lactate accumulated in the medium was reduced by ~30% compared with controls in

both the p53$^{+/+}$ and p53$^{-/-}$ cells. LDH-B silencing had no effect. This suggests that LDH-A silencing results in similar inhibition of aerobic glycolysis in HCT116 p53$^{+/+}$ and p53$^{-/-}$ cells (Figure 3a).

Both the HCT116 p53$^{+/+}$ and p53$^{-/-}$ cancer cells showed increased oxygen consumption following LDH-A silencing, suggesting increased oxidative metabolism to compensate for inhibition of aerobic glycolysis (Figure 3b). Under normal growth conditions, the p53$^{+/+}$ cancer cells showed slightly higher levels of oxygen consumption than the p53$^{-/-}$ cells, as has been reported previously.[30] Following LDH-A silencing, oxygen consumption increased in both the p53$^{+/+}$ and p53$^{-/-}$ cells (Figure 3b). This was unexpected for the p53$^{-/-}$ cancer cells as pyruvate entry into the tricarboxylic acid cycle is constitutively
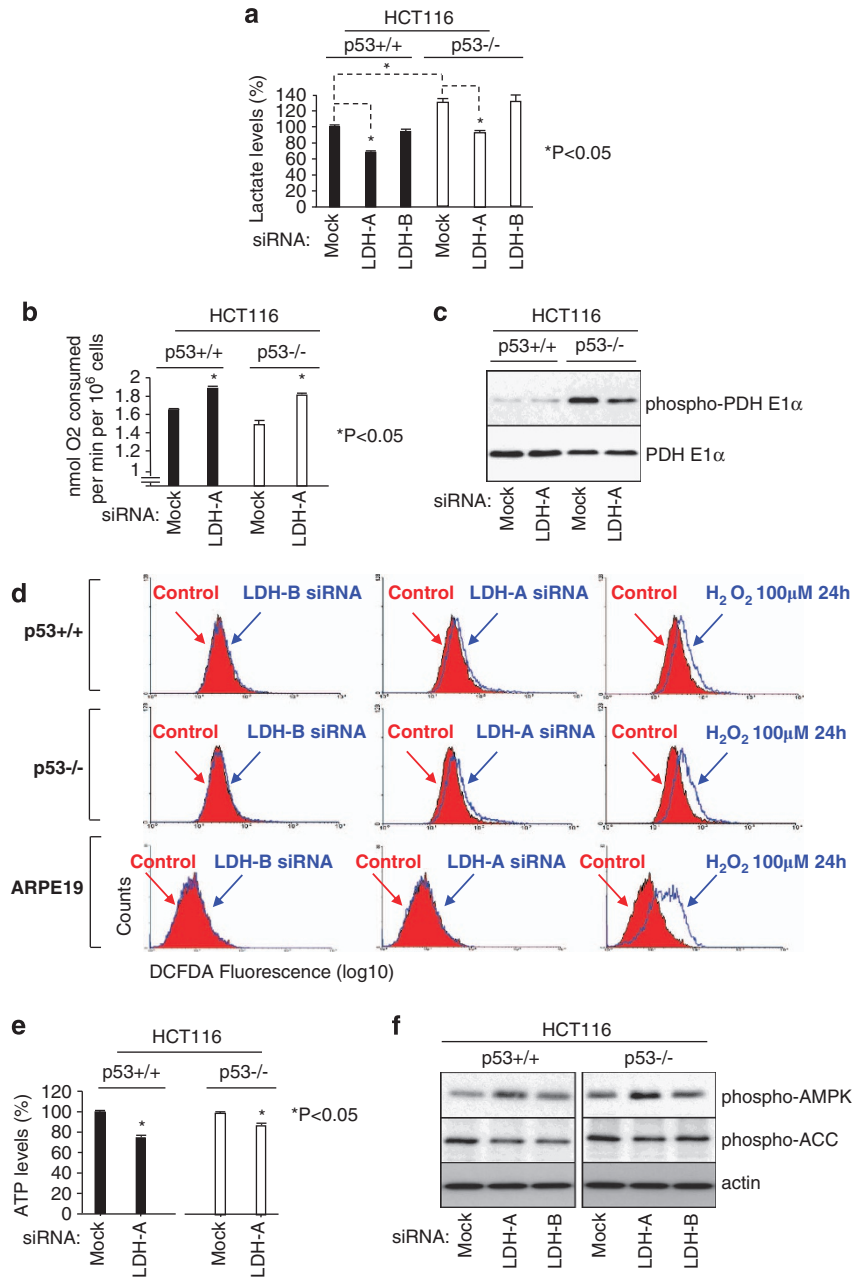
**Figure 3.** Effect of p53 upon the cellular metabolic response to LDH-A silencing. (**a**) Effects of LDH-A and LDH-B silencing on lactate production in HCT116 p53$^{+/+}$ and p53$^{-/-}$ cells, as assayed by levels of lactate accumulated in the culture medium 30 h after siRNA transfection (see Materials and methods). Statistical significance ($P < 0.05$) between LDH-A-silenced cells and control cells, and between HCT116 p53$^{+/+}$ cells and p53$^{-/-}$ cells is indicated by an asterisk. (**b**) Effects of LDH-A silencing on the rate of cellular oxygen consumption in HCT116 p53$^{+/+}$ and p53$^{-/-}$ cells 30 h after transfection as determined with a Clark-type oxygen electrode (see Materials and methods). Statistical significance ($P < 0.05$) between LDH-A-silenced cells and control cells is indicated by an asterisk. (**c**) Immunoblots showing levels of phosphorylated pyruvate dehydrogenase E1α (PDH E1α) in HCT116 p53$^{+/+}$ cells and p53$^{-/-}$ cells under normal growth conditions and following LDH-A silencing. For the representative blot shown, quantification by densitometry indicates a 2.7-fold decrease in phosphorylated PDH E1α in p53$^{-/-}$ cells following LDH-A silencing. (**d**) Effects of LDH-A or LDH-B silencing on intracellular ROS levels 48 h after siRNA transfection of HCT116 and ARPE19 cells. ROS levels were determined by flow cytometry and levels of DCFDA fluorescence (see Materials and methods). As a positive control for increased ROS, cells were treated with 100 μM H$_2$O$_2$ for 24 h. (**e**) Effects of LDH-A silencing on cellular ATP levels in HCT116 p53$^{+/+}$ and p53$^{-/-}$ cells 48 h after siRNA transfection. Statistical significance ($P < 0.05$) between LDH-A-silenced cells and control cells is indicated by an asterisk. (**f**) Effects of LDH-A and LDH-B silencing in HCT116 p53$^{+/+}$ and p53$^{-/-}$ cells on phosphorylation of AMPK (T172) and acetyl-CoA carboxylase (ACC) (S79) 48 h after siRNA transfection.

suppressed through phosphorylation and inactivation of the pyruvate dehydrogenase (PDH) complex by pyruvate dehydrogenase kinases.[31] Significantly, LDH-A silencing in the p53$^{-/-}$ cells caused an ~3-fold decrease in phosphorylated PDH (Figure 3c). This is likely to increase pyruvate metabolism by oxidative phosphorylation and increase oxygen consumption. This

identifies an important novel role for LDH-A, directly or indirectly, in the regulation of PDH phosphorylation state and activity. In contrast, LDH-A silencing had no effect on PDH phosphorylation in the p53$^{+/+}$ cells (Figure 3c), which are maintained at low levels by p53 via negative regulation of pyruvate dehydrogenase kinase 2 transcription.[32]

Oxidative phosphorylation generates reactive oxygen species (ROS).[33] Increased oxidative phosphorylation resulting from LDH-A knockdown could lead to more intracellular ROS, which are damaging to the cell and can cause cell death.[33,34] Indeed, LDH-A silencing resulted in a small but significant log increase in ROS in both the HCT116 p53^{+/+} and p53^{−/−} cells (Figure 3d). Importantly, LDH-B silencing had no effect on intracellular ROS levels (Figure 3d). In ARPE19 non-cancer cells, neither LDH-A nor LDH-B silencing had any effect on ROS levels (Figure 3d).

LDH-A silencing also caused a small decrease in adenosine triphosphate (ATP) levels in the HCT116 p53^{+/+} and p53^{−/−} cancer cells (Figure 3e), suggesting that despite increasing oxidative metabolism, the cells are unable to fully compensate bioenergetically. Consistent with this, LDH-A silencing also activated 5′-adenosine monophosphate-activated protein kinase (AMPK), as indicated by increased phosphorylated AMPK (Figure 3f). AMPK senses changes in cellular AMP/ATP and acts to increase ATP production by promoting catabolic reactions.[35] No increase was observed in phosphorylated acetyl-CoA carboxylase (ACC), an AMPK substrate that promotes B-oxidation (Figure 3f). In summary, LDH-A silencing in both the HCT116 p53^{+/+} and p53^{−/−} cancer cells results in increased oxidative and bio-energetic stress (increased ROS, reduced ATP), both of which may contribute to apoptosis. Superficially, the metabolic response to LDH-A silencing appeared similar in the isogenic p53^{+/+} and p53^{−/−} cancer cells and it is presently unclear why the increase in the cellular NADH/NAD^{+} ratio is p53-dependent. Future metabolomic analyses will investigate the mechanistic bases for this p53 dependency.

### LDH-A suppression reduces NAD^{+}-dependent SIRT1 activity in a p53-dependent manner

Using an in vitro SIRT1 deacetylase assay, the effect of suppressing LDH-A on SIRT1 activity was determined. We reasoned that the increase in cancer cell NADH:NAD^{+} ratio caused by suppressing LDH-A (Figure 2) might affect the activity of non-glycolytic NAD^{+}-dependent enzymes such as SIRT1. NHI-2 caused a dose-dependent decrease in SIRT1 activity in the HCT116 p53^{+/+} cells ($P < 0.05$) (Figure 4a). Importantly, in HCT116 p53^{−/−} cells, which fail to show any change in NADH:NAD^{+} in response to LDH-A suppression, there was no detectable effect of NHI-2 upon SIRT1 activity (Figure 4a). Significantly, for HCT116 p53^{+/+} cells treated with NHI-2, the addition of 2 mM NAD^{+} rescued SIRT1 activity (Figure 4a), demonstrating that the inhibitory effects of LDH-A suppression upon SIRT1 activity are due to its effects upon NADH:NAD^{+}. Silencing LDH-A by RNAi also reduced SIRT1 activity in HCT116 p53^{+/+} cancer cells (data not shown).

In HCT116 cancer cells, SIRT1 constitutively deacetylates p53 at K382[19] and SIRT1 silencing increases acetylated K382 p53 levels.[19] We therefore asked whether LDH-A silencing also increases acetylated K382 p53 levels. Significantly LDH-A silencing caused a marked increase in p53 K382 acetylation levels in HCT116 p53^{+/+} cancer cells consistent with reduced SIRT1 activity (Figure 4b). LDH-A silencing also increased the expression of p21, a downstream target of acetylated p53 (Figure 4c). It is unclear to what extent the reduction in SIRT1 activity might contribute to apoptosis in the HCT116 p53^{+/+} cancer cells. However, as reported previously,[19] SIRT1 silencing induces apoptosis in HCT116 p53^{+/+} cancer cells, an effect specifically rescued by Forkhead box protein O4 (Foxo4) cosilencing (Supplementary Figure S1). Interestingly, cosilencing Foxo4 with LDH-A in HCT116 p53^{+/+} cancer cells partially rescued apoptosis induced by LDH-A silencing (Supplementary Figure S1).

In non-cancer ARPE19 cells, acetylated K382 p53 remained undetectable following LDH-A depletion (presumably due to continued deacetylation by SIRT1)[19] (Figure 4b). SIRT1 silencing in
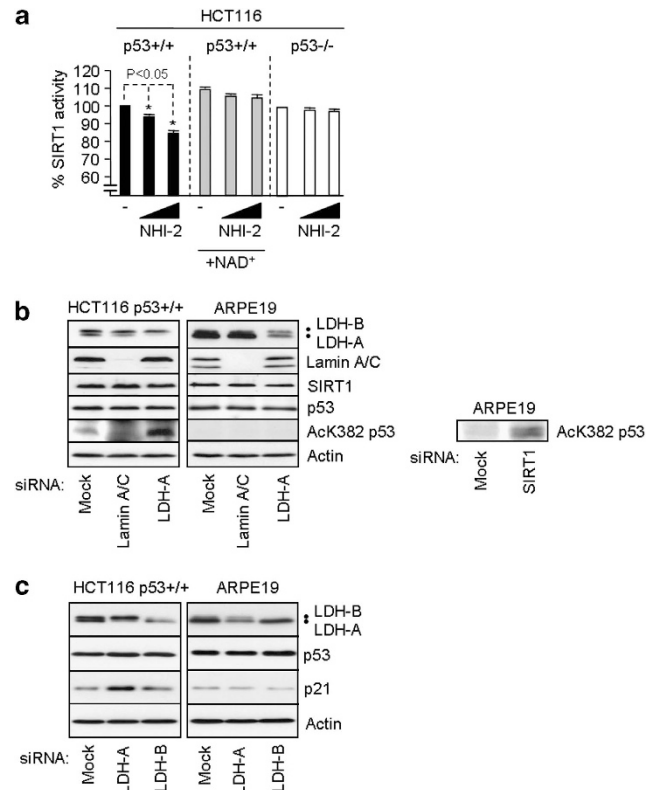


Figure 4. LDH-A suppression reduces SIRT1 activity in HCT116 p53^{+/+} cancer cells. (a) Effect of LDH-A inhibitor NHI-2 on SIRT1 activity in HCT116 p53^{+/+} and p53^{−/−} cancer cells. (6.125 and 12.5 μM NHI-2, 1 h 30 cell exposure) and rescue of reduced SIRT1 activity in HCT116 p53^{+/+} cells by 2 mM NAD^{+}. Statistical significance ($P < 0.05$) between NHI-2 treated cells and dimethyl sulfoxide (DMSO)-treated control cells is indicated by an asterisk. (b) Effect of LDH-A silencing on p53 acetylation levels at K382 in HCT116 cancer cells and ARPE19 non-cancer cells. Control immunoblots for total p53, SIRT1, lamin A/C and LDH-A are shown. ARPE19 panel (far right) indicates that p53 in ARPE19 cells can be acetylated at K382 and that it is subject to constitutive deacetylation by SIRT1. (c) Immunoblots showing induction of p21 expression by LDH-A silencing in HCT116 p53^{+/+} cancer cells, but not in ARPE19 non-cancer cells.

ARPE19 cells allows detection of p53 acetylated at K382 (Figure 4b, far-right panel), suggesting that in ARPE19 cells LDH-A silencing does not significantly alter SIRT1 activity. This is consistent with our observation that LDH-A knockdown has no effect on NADH:NAD^{+} in non-cancer ARPE19 cells (Figure 2a). LDH-A silencing also failed to induce p21 in ARPE19 cells, consistent with no effect on SIRT1 activity or p53 K382 deacetylation (Figures 4b and c).

These results provide proof-of-principle that suppressing LDH-A can provide a way of altering the activity of non-glycolytic NAD^{+}-dependent enzymes such as SIRT1 in a cancer-selective manner. Our results showing that suppressing LDH-A affects cancer cell SIRT1 activity are consistent with a recent study which reports that galloflavin, a novel inhibitor of both LDH isoforms (A and B),[36] reduces SIRT1 activity in Burkitt lymphoma cells.[37]

### LDH-A suppression enhances redox-dependent EO9-induced DNA damage in HCT116 p53^{+/+} cancer cells

We considered whether the increase in cancer cell NADH:NAD^{+} induced by LDH-A suppression could increase the activity of
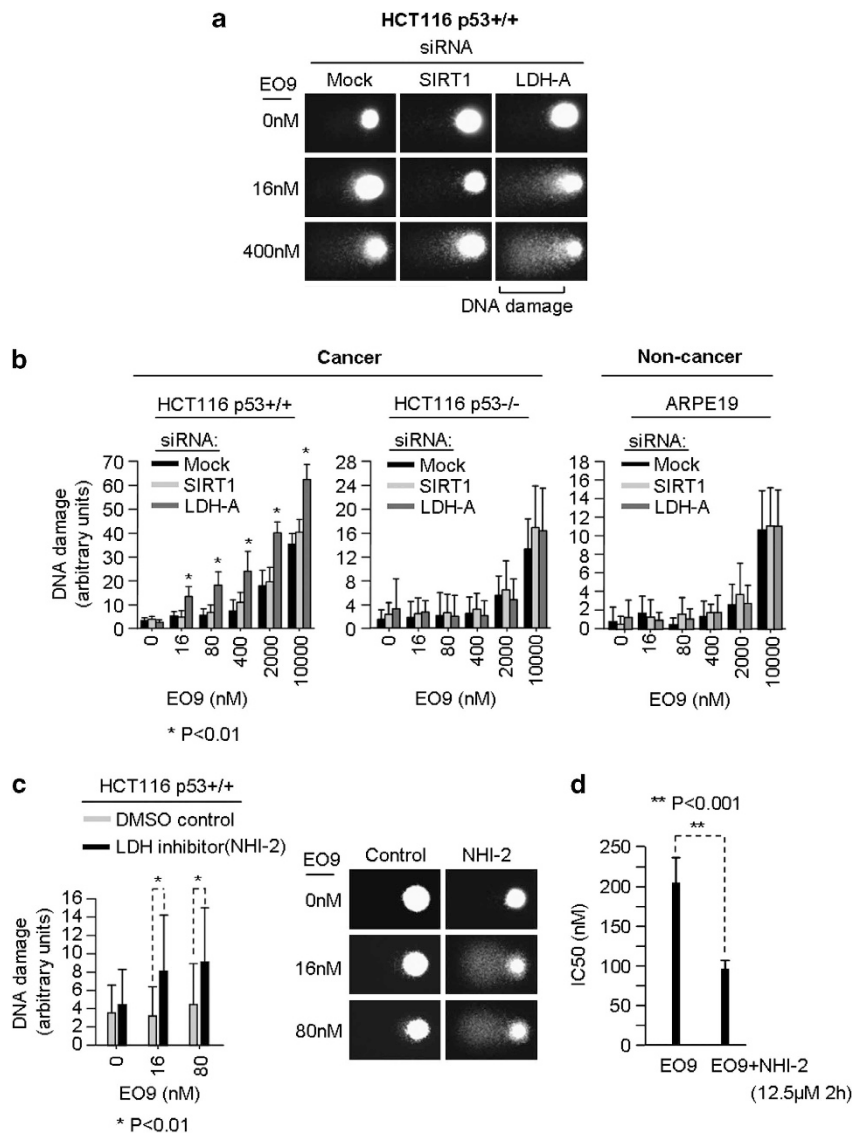
**Figure 5.** LDH-A suppression enhances DNA damage induced by the redox-sensitive anticancer drug EO9 in a p53-dependent, cancer-selective manner. (a) Representative comet images showing the effects of LDH-A or SIRT1 silencing on EO9-induced SSBs in HCT116 $p53^{+/+}$ cancer cells as determined by the alkaline comet assay. (b) Histograms showing the effects of LDH-A silencing on EO9-induced SSBs in HCT116 $p53^{+/+}$ and $p53^{-/-}$ cancer cells and ARPE19 non-cancer cells. Mean data ± s.d. from 50 comets. Statistical significance as determined by the Mann–Whitney *U*-test ($P < 0.01$) between LDH-A-silenced cells and control cells is indicated by an asterisk. (c) Histogram and comet images showing the effects of LDH-A inhibitor NHI-2 (12.5 μM 1 h pretreatment plus 1 h coincubation with EO9) on EO9-induced SSBs in HCT116 $p53^{+/+}$ cells. Statistical significance as determined by the Mann–Whitney *U*-test ($P < 0.01$) between NHI-2-treated cells and control cells is indicated by an asterisk. (d) Histogram showing the effects of NHI-2 on EO9 cytotoxicity in HCT116 $p53^{+/+}$ cancer cells, as indicated by $IC_{50}$ values. Cells were treated for 1 h with NHI-2 to modulate cancer cell NADH:NAD$^+$ ratio before 1 h coincubation with EO9. Cells were then incubated in fresh media for 4 days and effects on cell survival determined. Minimum of $n = 3$ experiments, statistical significance (**$P < 0.001$) is indicated.

cellular NADH-dependent enzymes. For this, we focused on NAD(P)H-dependent oxidoreductase NQO1, which activates the anticancer prodrug EO9 to induce single-strand DNA breaks (SSBs).[15–17] In a cell-free assay, induction of SSBs in plasmid DNA by EO9 was directly proportional to NADH concentration (Supplementary Figure S3a). The effects of silencing LDH-A or SIRT1 on the ability of EO9 to cause SSBs in cells were determined using the alkaline comet assay.[38] EO9 induced SSBs in a dose-dependent manner (Figures 5a and b), although interestingly HCT116 $p53^{+/+}$ cells appeared more susceptible to damage than isogenic HCT116 $p53^{-/-}$ cells and ARPE19 cells despite similar NQO1 levels (Supplementary Figure S3b). Quantification of DNA damage, by analysis of tail moments, demonstrated that levels of

EO9-induced DNA damage in SIRT1-silenced cells were equivalent to controls. Importantly, in LDH-A-silenced HCT116 $p53^{+/+}$ cells, the extent of DNA damage was considerably and significantly higher at each EO9 dose compared with SIRT1-silenced cells and controls (Figures 5a and b; $P < 0.01$). In contrast, no increase in EO9-induced SSBs was observed in HCT116 $p53^{-/-}$ cells or ARPE19 non-cancer cells following LDH-A silencing (Figure 5b). This is consistent with the NADH dependency of EO9 activity and LDH-A silencing increasing NADH:NAD$^+$ in $p53^{+/+}$ cancer cells, but not in $p53^{-/-}$ or ARPE19 cells. Brief treatment with LDH-A inhibitor NHI-2 to increase cancer cell NADH/NAD$^+$ ratio (Figure 2b) followed by 1 h coincubation with EO9 also significantly enhanced EO9-induced SSBs in HCT116 $p53^{+/+}$ cells

(Figure 5c; $P < 0.01$). NHI-2 also enhanced EO9-induced SSBs in HCT116 p53$^{-/-}$ cells transiently transfected with p53 relative to control transfections (Supplementary Figure S3c). These results suggest that LDH-A suppression (via increased NADH:NAD$^+$) can increase NAD(P)H-dependent NQO1 activity and this is associated with an increase in DNA damage induction by EO9, the overall process being p53-dependent.

NHI-2 potentiates EO9 cytotoxicity and induces cancer cell death
We next asked whether brief cellular exposure to NHI-2 to modulate NADH/NAD$^+$ and enhance EO9-induced DNA damage has any effect on EO9-induced cancer cell death. HCT116 p53$^{+/+}$ cancer cells were exposed to 12.5 μM NHI-2 for 1 h and then a further 1 h with EO9 (0–2500 nM EO9, twofold dilution series) before washout and incubation of cells in fresh media for 4 days. Using the MTT assay, IC$_{50}$ values were then determined and significantly NHI-2 plus EO9 caused a twofold reduction in the IC$_{50}$ compared with EO9 alone (Figure 5d). NHI-2 alone of 12.5 μM (2 h exposure) had no effect on cell growth or survival, indicating that potentiation of EO9 is not due to cytotoxicity of NHI-2 (Supplementary Figure S3d). Importantly, more prolonged inhibition of LDH-A by NHI-2 (48 h, 35 μM) caused significant apoptosis in both HCT116 p53$^{+/+}$ and p53$^{-/-}$ cancer cells, but not in ARPE19 non-cancer cells (Supplementary Figure S4). Significantly, NHI-2 induced more apoptosis in the p53$^{+/+}$ cancer cells than in the p53$^{-/-}$ cancer cells (Supplementary Figure S4). These results,

consistent with those obtained by RNAi (Figure 1), identify two potential therapeutic applications of LDH-A inhibitors: (i) as a single agent, for targeting both p53$^{+/+}$ and p53$^{-/-}$ cancer cells and (ii) through synergy with redox-dependent anticancer agents (via NADH:NAD$^+$, p53$^{+/+}$ cancer cells only) (Figure 6).

## DISCUSSION
There is a need for more targeted therapeutic approaches with fewer adverse side effects. In this context, LDH-A is an attractive target to consider because of its cancer-selective role. This work identifies two distinct mechanisms by which LDH-A inhibitors could potentially be used to kill cancer cells selectively, (i) through apoptosis induction, irrespective of cancer cell p53 status and (ii) as a part of a combinatorial therapeutic approach via a p53/NAD(H)-dependent mechanism (Figure 6).

Suppressing LDH-A *in vitro* was sufficient to induce significant cancer cell death by apoptosis. Importantly, this was independent of cellular p53 status as apoptosis was induced in p53 wild-type, p53-mutant and p53-null cancer cell lines. This is significant as p53 is a key regulator of multiple aspects of cellular metabolism including the Warburg effect;[6] furthermore, the effectiveness of many current cancer treatments is dependent on wild-type p53.

LDH-A suppression perturbed the cellular balance of NADH/NAD$^+$ selectively in p53$^{+/+}$ cancer cells. This uncovers an important novel role for p53 in the regulation of cancer cell NADH/NAD$^+$ following LDH-A targeting. Future metabolomic and
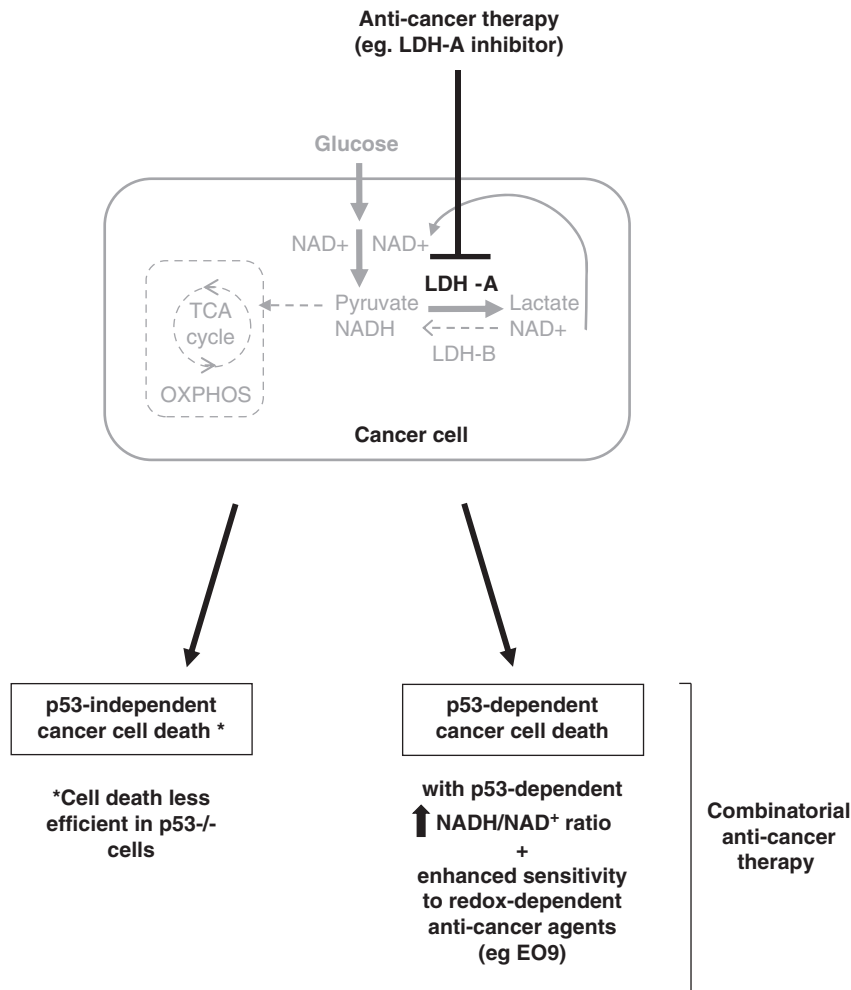


**Figure 6.** LDH-A and anticancer therapy: p53-dependent and p53-independent routes to cancer cell death. Schematic based on our results summarising opportunities for anticancer therapy via LDH-A targeting.

metabolic flux analyses will investigate the mechanistic basis for this p53 dependency. We further show that altering cancer cell $NADH:NAD^+$, via LDH-A/p53, provides a potential strategy for altering the activity of non-glycolytic NAD(H)-dependent enzymes. Indeed, by suppressing LDH-A, we were able to reduce $NAD^+$-dependent SIRT1 deacetylase activity selectively in $p53^{+/+}$ cancer cells, resulting in increased acetylated p53. Excess $NAD^+$ rescued SIRT1 activity, linking the effect on SIRT1 activity to LDH-A-mediated modulation of cancer cell $NADH:NAD^+$.

The increase in cancer cell $NADH:NAD^+$ caused by LDH-A suppression also appeared to increase the activity of the NADH-dependent enzyme NQO1, which activates the anticancer prodrug EO9.[15–17] LDH-A suppression increased EO9-induced DNA damage in a p53-dependent, cancer-selective manner and reduced its $IC_{50}$ twofold. EO9 has completed phase II clinical trials for treating superficial bladder cancer.[39,40] As p53 mutations are rare in these tumours,[41] LDH-A inhibition could potentially enhance the therapeutic index of EO9 for such tumours.

The major difficulty with chemotherapy and most combinational approaches is how to increase toxicity toward cancer cells without increasing damage to normal cells. Here, we show that, via LDH-A/p53 and cancer-specific NAD(H) modulation, it may be possible to enhance the efficacy of certain redox-dependent chemotherapeutic agents such as EO9 selectively in p53-wild type cancer cells without parallel sensitisation of non-cancer cells.

Thus, by exploiting the altered metabolism of cancer cells, as reported here by targeting LDH-A, this may offer novel opportunities for selective therapeutic targeting of cancer cells, either as a monotherapy or as part of a combinatorial approach (Figure 6).

## MATERIALS AND METHODS

### Cell lines
All cell lines were authenticated, maintained at low passage and cultured in antibiotic-free media. $p53^{+/+}$ and $p53^{-/-}$ isogenic clones of HCT116 human colorectal epithelial cancer cells[42] of <3 passages were used to study p53-related effects. Other human colorectal cancer cell lines used were LS174, LoVo (both p53 wild-type) and DLD1 (mutant p53, S241F). Other cancer cell lines used were MCF7 (p53 wild-type), MDA-MB-231 (mutant p53, R280K) and MDA-MB-468 (mutant p53, R273H) breast cancer cells, SAOS2 (osteosarcoma, p53-null) and SiHa (cervical carcinoma, p53-null). SiHa contain one to two integrated copies of the HPV16 genome per cell and are functionally p53-null due to the expression of HPV16 E6. Non-cancer cells were ARPE19 human retinal epithelial cells, which senesce after >8 passages,[43] and WI38 normal human diploid lung fibroblasts.

### siRNA transfection
Cells were transfected by formulating HPLC-purified synthetic siRNAs into liposomes as described previously.[19,44] Two independent LDH-A siRNAs were designed that target different exons of the LDH-A mRNA. Both LDH-A siRNAs gave similar results and efficiently silenced LDH-A: LDHA siRNA 1 (5′-CCAGCCGUGAUAAUGACCA(dTdT)-3′); LDHA siRNA 2 (5′-GGAGUGGAA UGAAUGUUGC(dTdT)-3′). Unless stated otherwise, the data shown were generated with LDHA siRNA 1. LDH-B siRNA (5′-ACUUAAUCCAAUAGCCCAG (dTdT)-3′). Lamin A/C, SIRT1 and Foxo4 siRNAs were as published.[19] siRNA selectivity and silencing efficiency was confirmed by the assessment of target and non-target mRNA levels by qRT-PCR as described previously.[19,44]

### mRNA quantification
Total cellular RNA was isolated as described[44] and used for quantitative real-time RT–PCR on a DNA Engine Opticon2 system using Quantitect SYBRGreen RT–PCR Kit (Qiagen, Hilden, Germany). For LDH-A mRNA quantification primers. 5′-TTGGTCCAGCGTAACGTGAAC-3′ and 5′-CCAG-GATGTGTAGCCTTTGAG-3′ were used in the thermal cycle: 50 °C for 30 min, 94 °C for 15 min, followed by 36 cycles of 94 °C for 30 s, 55 °C for 30 s, 72 °C for 45 s. For LDH-B, primers 5′-CTGGGAAAGTCTCTGGCTGATG-3′ and 5′-CA CTCCACACAGCCACACTTGA-3′ were used under identical cycling

conditions. except that primer annealing was at 60 °C for 30 s. Cycle parameters and primers for SIRT1 and lamin A/C were as described.[19]

### DNA transfection
For DNA transfection, HCT116 cells were seeded in six-well plates at $2.4 \times 10^5$ cells per well. Cells were transfected with 250 ng pcDNA3.1 expression plasmid encoding human wild-type p53 under the control of the cytomegalovirus promoter (pcDNA3.1 WTp53) or pcDNA3.1 empty vector as a negative control.

### NAD(H) quantification
An enzymatic cycling reaction was used for the quantification of cellular $NAD^+$ and NADH, as described.[45] $NAD^+$ and NADH concentrations were normalised relative to protein concentration (µM NAD(H)/mg protein). Results were expressed graphically as the fold-change in $NADH/NAD^+$ ratio relative to mock-transfected cells.

### Statistical analysis
Statistical analysis was carried out using a two-tailed Student's t-test or the Mann–Whitney U-test (Figure 5). A P-value of <0.05 was considered statistically significant.

### Immunoblotting
Cell extracts were prepared as described[46] and equivalent amounts resolved by sodium dodecyl sulfate–polyacrylamide gel electrophoresis and electroblotted onto nitrocellulose for immunoblotting. Primary antibodies were: anti-LDH (Epitomics, Burlingame, CA, USA; antibody detects both LDH-A and LDH-B: see Figure 1b), anti-SIRT1 (Santa Cruz, Biotechnology, Santa Cruz, CA, USA), anti-p53 (Santa Cruz), anti-acetylated K382 p53 (Epitomics), anti-p21 (BD Biosciences, San Jose, CA, USA), anti-PDH-E1α (Abcam, Cambridge, UK), anti-phosphorylated S293 PDH-E1α (Novus Biologics, Littleton, CO, USA), antiphosphorylated T172 AMPK (Cell Signaling Technology, Beverly, MA, USA) antiphosphorylated S79 acetyl-CoA carboxylase (Cell Signalling Technology), anti-lamin A/C (Santa Cruz) and anti-actin (Chemicon International, Temecula, CA, USA).

### Apoptosis quantification
Apoptotic cells were identified by flow cytometry using Annexin-V-Fluos (Roche, Penzberg, Germany) following the manufacturer's protocol as described previously.[44]

### Determination of lactate and ATP levels
Lactate levels in the culture media of cells were determined using a Lactate Assay Kit (Biovision Inc., Milpitas, CA, USA; no. K607) as described by the manufacturer's instructions. Cellular ATP levels were determined using an ATP Bioluminescence Kit (Roche). Lactate and cellular ATP levels were determined 30 h after siRNA transfection and values were normalised to cell number.

### Oxygen consumption and ROS measurement
Cellular oxygen consumption was measured 30 h after siRNA transfection using a Clark-type oxygen electrode (Oxytherm; Hansatech Instruments Ltd, Norfolk, UK). Oxygen consumption rates were measured over a 20 min linear period and normalised to cell number. Levels of intracellular ROS were determined using flow cytometry following 30 min incubation of cells with 5 µM carboxy-$H_2$DCFDA (Invitrogen, Carlsbad, CA, USA; C-400), a cell-permeant reduced fluorescein derivative oxidised by ROS to produce fluorescence. As a positive comparative control for increased ROS, cells were treated with 100 µM $H_2O_2$ for 24 h and incubated with carboxy-$H_2$DCFDA.

### SIRT1 deacetylase assay
SIRT1 activity of cell extracts was measured using a fluorometric in vitro SIRT1 deacetylase assay (Abnova, Taipei, Taiwan) as described previously[47] and in accordance with the manufacturer's protocol. The assay was performed in the presence of trichostatin A to inhibit any nonspecific deacetylation of the SIRT1 substrate by other deacetylases present. The assay was carried out in the absence of any added $NAD^+$ as it was presumed that any effects of LDH-A suppression on cellular SIRT1 activity would be due to effects of LDH-A on cellular $NAD^+$ levels. This was directly

tested and confirmed, as shown in Figure 4a, by the addition of 2 mM $NAD^+$ to the reactions.

## Comet assay analysis of DNA damage following EO9 treatment

At 30 h after siRNA transfection, cells were exposed to a range of EO9 concentrations (0–10 μM) for 1 h. Induction of single-strand DNA breaks was determined using the alkaline comet assay as described previously.[38] Comets were visualised using an epifluorescent microscope and images were analysed using Comet Assay III software (Perceptive Instruments, Bury St. Edmunds, UK). Fifty comets were randomly selected and tail moments were obtained.

## Influence of NADH on induction of single-strand breaks in plasmid DNA by EO9

Induction of single-strand DNA breaks following reduction of EO9 by NQO1 was determined by measuring conversion of supercoiled plasmid DNA to open circular DNA as described.[48] Each reaction contained 10 μM EO9, 1 μg/ml purified recombinant NQO1, 2 μg plasmid and NADH (2 mM–0.031 mM). Following 1 h at 37 °C, the reaction was terminated and DNA separated on a 1% Tris-acetate-EDTA-agarose gel.

## Measurement of NQO1 activity

As a measure of NQO1 levels, the specific activity of NQO1 in the presence of excess NADH (2 mM) was determined by measuring the dicumarol-sensitive reduction of DCPIP as described previously.[49]

## Chemosensitivity studies

$HCT116^{+/+}$ cells were seeded in 96-well plates at $1 \times 10^3$ cells per well. The following day, cells were incubated in media containing 12.5 μM NHI-2 for 1 h. Cells were then incubated with media containing 12.5 μM NHI-2 and EO9 at a range of concentrations (0–2.5 μM) for a further 1 h. Cells were then washed with phosphate-buffered saline before the addition of normal growth media. Cells were then incubated for 4 days before cell survival was determined using the MTT assay.[50] Two controls were used: no EO9 or NHI-2, and 12.5 μM NHI-2 only. Another plate was set up and exposed to EO9 only. Percentage cell survival was determined as the absorbance of treated cells divided by the absorbance of controls × 100. $IC_{50}$ values were determined and statistical analysis was performed using a two-tailed Student's t-test.

## CONFLICT OF INTEREST

The authors declare no conflict of interest.

## REFERENCES

1 Hanahan D, Weinberg RA. Hallmarks of cancer: the next generation. Cell 2011; 144: 646–674.

2 Deberardinis RJ, Sayed N, Ditsworth D, Thompson CB. Brick by brick: metabolism and tumor cell growth. Curr Opin Genet Dev 2008; 18: 54–61.

3 Vander Heiden MG, Cantley LC, Thompson CB. Understanding the Warburg effect: the metabolic requirements of cell proliferation. Science 2009; 324: 1029–1033.

4 Knight JR, Milner J. SIRT1 metabolism and cancer. Curr Opin Oncol 2012; 24: 68–75.

5 Dang CV, Semenza GL. Oncogenic alterations of metabolism. Trends Biochem Sci 1999; 24: 68–72.

6 Vousden KH, Ryan KM. P53 and metabolism. Nat Rev Cancer 2009; 9: 691–700.

7 Markert CL, Shaklee JB, Whitt GS. Evolution of a gene. Multiple genes for LDH isozymes provide a model of the evolution of gene structure, function and regulation. Science 1975; 189: 102–114.

8 Read JA, Winter VJ, Eszes CM, Sessions B, Bradly RL. Structural basis for altered activity of M- and H-isozyme forms of human lactate dehydrogenase. Proteins 2001; 43: 175–185.

9 Fantin VR, St-Pierre J, Leder P. Attenuation of LDH-A expression uncovers a link between glycolysis, mitochondrial physiology, and tumor maintenance. Cancer Cell 2006; 9: 425–434.

10 Xie H, Valera VA, Merino MJ, Amato AM, Signoretti S, Linehan WM et al. LDH-A inhibition, a therapeutic strategy for treatment of hereditary leiomyomatosis and renal cell cancer. Mol Cancer Ther 2009; 8: 626–635.

11 Le A, Cooper CR, Gouw AM, Dinavahi R, Maitra A, Deck LM et al. Inhibition of lactate dehydrogenase A induces oxidative stress and inhibits tumor progression. Proc Natl Acad Sci USA 2010; 107: 2037–2042.

12 Lin SJ, Guarente L. Nicotinamide adenine dinucleotide, a metabolic regulator of transcription, longevity and disease. Curr Opin Cell Biol 2003; 15: 241–246.

13 Khan JA, Forouhar F, Tao X, Tong L. Nicotinamide adenine dinucleotide metabolism as an attractive target for drug discovery. Expert Opin Ther Targets 2007; 11: 695–705.

14 Zhang T, Berrocal JG, Frizzell KM, Gamble MJ, DuMond ME, Krishnakumar R et al. Enzymes in the $NAD^+$ salvage pathway regulate SIRT1 activity at target gene promoters. J Biol Chem 2009; 284: 20408–20417.

15 Workman P. Enzyme-directed bioreductive drug development revisited: a commentary on recent progress and future prospects with emphasis on quinone anticancer agents and quinone metabolising enzymes, particularly DT-diaphorase. Oncol Res 1994; 6: 461–475.

16 Butler J, Spanswick VJ, Cummings J. The autoxidation of the reduced forms of EO9. Free Radic Res 1996; 25: 141–148.

17 Cadenas E. Antioxidant and prooxidant functions of DT-diaphorase in quinone meta. Biochem Pharmacol 1995; 49: 127–140.

18 North BJ, Verdin E. Sirtuins: Sir2-related NAD-dependent protein deacetylases. Genome Biol 2004; 5: 224.

19 Ford J, Jiang M, Milner J. Cancer-specific functions of SIRT1 enable human epithelial cancer cell growth and survival. Cancer Res 2005; 65: 10457–10463.

20 Yamakuchi M, Ferlito M, Lowenstein CJ. miR-34a repression of SIRT1 regulates apoptosis. Proc Natl Acad Sci USA 2008; 105: 13421–13426.

21 Chen J, Zhang B, Wong N, Lo AW, To KF, Chan AW et al. Sirtuin 1 is upregulated in a subset of hepatocellular carcinomas where it is essential for telomere maintenance and tumor cell growth. Cancer Res 2011; 71: 4138–4149.

22 Zhao G, Cui J, Zhang JG, Qin Q, Chen Q, Yin T et al. SIRT1 RNAi knockdown induces apoptosis and senescence, inhibits invasion and enhances chemosensitivity in pancreatic cancer cells. Gene Ther 2011; 18: 920–928.

23 von Heideman A, Berglund A, Larsson R, Nygren P. Safety and efficacy of NAD depleting cancer drugs: results of a phase I clinical trial of CHS 828 and overview of published data. Cancer Chemoth Pharm 2010; 65: 1165–1172.

24 Luo J, Nikolaev AY, Imai S, Chen D, Su F, Shiloh A et al. Negative control of p53 by Sir2alpha promotes cell survival under stress. Cell 2001; 107: 137–148.

25 Vaziri H, Dessain SK, Ng Eaton E, Imai SI, Frye RA, Pandita TK et al. hSIR2(SIRT1) functions as an NAD-dependent p53 deacetylase. Cell 2001; 107: 149–159.

26 Tang Y, Zhao W, Chen Y, Zhao Y, Gu W. Acetylation is indispensable for p53 activation. Cell 2008; 133: 612–626.

27 Li T, Kon N, Jiang L, Tan M, Ludwig T, Zhao Y et al. Tumor suppression in the absence of p53-mediated cell-cycle arrest, apoptosis, and senescence. Cell 2012; 149: 1269–1283.

28 Granchi C, Calvaresi EC, Tuccinardi T, Paterni I, Macchia M, Martinelli A et al. Assessing the differential action on cancer cells of LDH-A inhibitors based on the N-hydroxyindole-2-carboxylate (NHI) and malonic (Mal) scaffolds. Org Biomol Chem 2013; 11: 6588–6596.

29 Granchi C, Roy S, Giacomelli C, Macchia M, Tuccinardi T, Martinelli A et al. Discovery of N-hydroxyindole-based inhibitors of human lactate dehydrogenase isoform A (LDH-A) as starvation agents against cancer cells. J Med Chem 2011; 54: 1599–1612.

30 Matoba S, Kang JG, Patino WD, Wragg A, Boehm M, Gavrilova O et al. P53 regulates mitochondrial respiration. Science 2006; 312: 1650–1653.

31 Kim JW, Dang CV. Cancer's molecular sweet tooth and the Warburg effect. Cancer Res 2006; 66: 8927–8930.

32 Contractor T, Harris CR. P53 negatively regulates transcription of the pyruvate dehydrogenase kinase Pdk2. Cancer Res 2012; 72: 560–567.

33 Brand KA, Hermfisse U. Aerobic glycolysis by proliferating cells: a protective strategy against reactive oxygen species. FASEB J 1997; 11: 388–395.

34 Gruning NM, Ralser M. Cancer: sacrifice for survival. Nature 2011; 480: 190–191.

35 Hardie DG, Ross FA, Hawley SA. AMPK: a nutrient and energy sensor that maintains energy homeostasis. Nat Rev Mol Cell Biol 2012; 13: 251–262.

36 Manerba M, Vettraino M, Fiume L, Di Stefano G, Sartini A, Giacomini E et al. Galloflavin (CAS 568-80-9): a novel inhibitor of lactate dehydrogenase. Chem Med Chem 2012; 7: 311–317.

37 Vettraino M, Manerba M, Govoni M, Di Stefano G. Galloflavin suppresses lactate dehydrogenase activity and causes MYC downregulation in Burkitt lymphoma cells through NAD/NADH-dependent inhibition of sirtuin-1. Anticancer Drugs 2013; 24: 862–870.

38 Phillips RM, Ward TH. Influence of extracellular pH on the cytotoxicity and DNA damage of a series of indolequinone compounds. *Anticancer Res* 2001; **21**: 1795–1801.

39 Puri R, Palit V, Loadman PM, Flannigan M, Shah T, Choudry GA *et al*. Phase I/II pilot study of intravesical apaziquone (EO9) for superficial bladder cancer. *J Urol* 2006; **176**: 1344–1348.

40 van der Heijden AG, Moonen PM, Cornel EB, Vergunst H, de Reijke TM, van Boven E *et al*. Phase II marker lesion study with intravesical instillation of apaziquone for superficial bladder cancer: toxicity and marker response. *J Urol* 2006; **176**: 1349–1353, discussion 1353.

41 Knowles MA. Molecular pathogenesis of bladder cancer. *Int J Clin Oncol* 2008; **13**: 287–297.

42 Bunz F, Dutriaux A, Lengauer C, Waldman T, Zhou S, Brown JP *et al*. Requirement for p53 and p21 to sustain G2 arrest after DNA damage. *Science* 1998; **282**: 1497–1501.

43 Dunn KC, Aotaki-Keen AE, Putkey FR, Hjelmeland LM. ARPE-19 a human retinal pigment epithelial cell line with differentiated properties. *Exp Eye Res* 1996; **62**: 155–169.

44 Allison SJ, Milner J. SIRT3 is pro-apoptotic and participates in distinct basal apoptotic pathways. *Cell Cycle* 2007; **6**: 2669–2677.

45 Umemura K, Kimura H. Determination of oxidized and reduced nicotinamide adenine dinucleotide in cell monolayers using a single extraction procedure and a spectrophotometric assay. *Anal Biochem* 2005; **338**: 131–135.

46 Ford J, Ahmed S, Allison S, Jiang M, Milner J. JNK2-dependent regulation of SIRT1 protein stability. *Cell Cycle* 2008; **7**: 3091–3097.

47 Lynch CJ, Shah ZH, Allison SJ, Ahmed SU, Ford J, Warnock LJ *et al*. SIRT1 undergoes alternative splicing in a novel auto-regulatory loop with p53. *PLoS ONE* 2010; **5**: e13502.

48 Phillips RM, Naylor MA, Jaffar M, Doughty SW, Everett SA, Breen AG *et al*. Bioreductive activation of a series of indolequinones by human DT-diaphorase: structure-activity relationships. *J Med Chem* 1999; **42**: 4071–4080.

49 Phillips RM. Bioreductive activation of a series of analogues of 5-aziridinyl-3-hydroxymethyl-1-methyl-[1H-indole-4, 7-dione] prop-beta-en-alpha-ol (EO9) by human DT-diaphorase. *Biochem Pharmacol* 1996; **52**: 1711–1718.

50 Phillips RM, Hulbert PB, Bibby MC, Sleigh NR, Double JA. *In vitro* activity of the novel indoloquinone EO-9 and the influence of pH on cytotoxicity. *Br J Cancer* 1992; **65**: 359–364.

Supplementary Information accompanies this paper on the Oncogenesis website (http://www.nature.com/oncsis).